

Helical Assembly through Charged Hydrogen Bonds in Aqueous Solvent

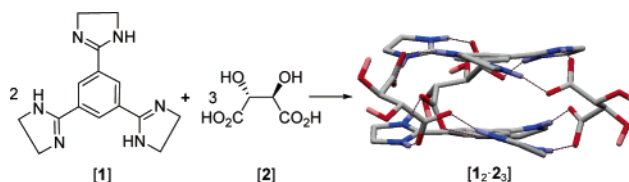
Hae-Jo Kim,[†] Shigeru Sakamoto,[‡] Kentaro Yamaguchi,[‡] and Jong-In Hong^{*,†,§}

School of Chemistry, College of Natural Sciences, Seoul National University, Seoul 151-747, Korea, Chemical Analysis Center, Chiba University, Chiba 263-8522, Japan, and Center for Molecular Design and Synthesis, KAIST, Daejeon 305-701, Korea

jihong@plaza.snu.ac.kr

Received January 28, 2003

ABSTRACT



Helical capsule-like assembly of $[1_2\cdot 2_3]$ shows a strong Cotton effect from the chirality transfer of the tartaric acid unit to tris(imidazolinium) base through charged hydrogen bonds in aqueous solvent.

Self-assembled supramolecules produced through noncovalent interactions are important for their possible applications to information storage, catalysis, molecular transport, separation, and sensing.¹ Most of those assembled by hydrogen bonding have been reported in apolar, noncompetitive solvents,² but self-assembled cage-like structures in polar solvents are less common.³ Moreover, H-bond mediated self-assembled chiral supramolecules in aqueous solvent⁴ are even less reported even though they exist in many biomolecules such as DNA and proteins. Herein we report a self-assembled

helical capsule-like structure, composed of two tris(imidazolinium) (**1**) bases and three tartaric acids through charged H-bonds in aqueous solution.

The pK_a value of the protonated form of **1**^{5b} is high (9.88) enough to play a role as a base. Thus, **1** can abstract protons from carboxylic acids.⁵ A 2:3 mixture of **1** and tartaric acid (**2**) is expected to form a self-assembled structure via proton transfer from the acids to the imidazolines. We expect that the charged, directional hydrogen bonding interactions between the tris(imidazolium) and tartrates would force both partners to form a discrete capsule-like structure with helicity directed by the chirality of tartaric acid (Scheme 1).

[†] Seoul National University.

[‡] Chiba University.

[§] Center for Molecular Design and Synthesis.

(1) (a) Kang, J.; Santamaría, J.; Hilmersson, G.; Rebek, J., Jr. *J. Am. Chem. Soc.* **1998**, *120*, 7389–7390. (b) Yoshizawa, M.; Takeyama, Y.; Kusakawa, T.; Fujita, M. *Angew. Chem., Int. Ed.* **2002**, *41*, 1347–1349. (c) Sánchez-Quesada, J.; Kim, H. S.; Ghadiri, M. R. *Angew. Chem., Int. Ed.* **2001**, *40*, 2503–2509. (d) Sancenón, F.; Martínez-Mañez, R.; Soto, J. *Angew. Chem., Int. Ed.* **2002**, *41*, 1416–1419.

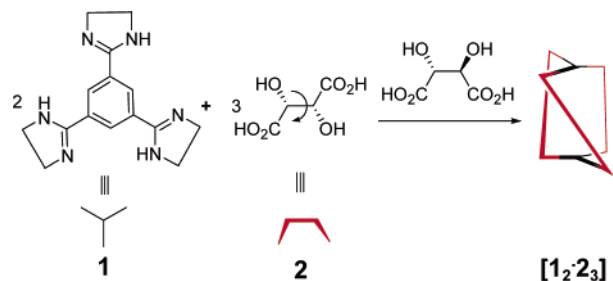
(2) (a) Kang, J.; Rebek, J., Jr. *Nature* **1996**, *382*, 239. (b) Ishi-i, T.; Crego-Calama, M.; Timmerman, P.; Reinhoudt, D. N.; Shinkai, S. *Angew. Chem., Int. Ed.* **2002**, *41*, 1924–1929. (c) MacGillivray, L. R.; Atwood, J. L. *Nature* **1997**, *389*, 469–472.

(3) (a) Lee, S. B.; Hong, J.-I. *Tetrahedron Lett.* **1996**, *37*, 8501–8504. (b) Hirschberg, J. H. K. K.; Brunsveld, L.; Lamzi, A.; Vekemans, J. A. J. M.; Sijbesma, R. P.; Meijer, E. W. *Nature* **2000**, *407*, 167–170. (c) Brewster, R. E.; Shuker, S. B. *J. Am. Chem. Soc.* **2002**, *124*, 7902–7903. (d) Corbellini, F.; Fiammengo, R.; Timmerman, P.; Crego-Calama, M.; Versluis, K.; Heck, A. J. R.; Luyten, I.; Reinhoudt, D. N. *J. Am. Chem. Soc.* **2002**, *124*, 6569–6575.

(4) For self-assembled nanotubes in aqueous solvent, see: (a) Ghadiri, M. R.; Granja, J. R.; Milligan, R. A.; McRee D. E.; Khazanovich, N. *Nature* **1993**, *366*, 324–327. For self-assembled nanotubes in polar solvent, see: (b) Fenniri, H.; Deng, B.-L.; Ribbe, A. E. *J. Am. Chem. Soc.* **2002**, *124*, 11064–11072. For self-assembled capsules in polar solvent, see: (c) Vysotsky, M. O.; Thondorf, I.; Böhmer, V. *Chem. Commun.* **2001**, 1890–1891. (d) Shivanyuk, A.; Rebek, J., Jr. *Chem. Commun.* **2001**, 2374–2375. (e) Atwood, J. L.; Barbour, L. J.; Jerga, A. *Chem. Commun.* **2001**, 2376–2377. For self-assembled capsules in water, see: (f) Hamelin, B.; Jullien, L.; Derouet, C.; du Penhoat, C. H.; Berthault, P. *J. Am. Chem. Soc.* **1998**, *120*, 8438–8447. (g) Grawe, T.; Schrader, T.; Zadmand, R.; Kraft, A. *J. Org. Chem.* **2002**, *67*, 3755–3763.

(5) (a) Félix, O.; Hosseini, M. W.; De Cian, A.; Fisher, J. *Angew. Chem., Int. Ed.* **1997**, *36*, 102–104. (b) Kraft, A.; Osterod, F. *J. Chem. Soc., Perkin Trans. 1* **1998**, 1019–1025. (c) Kraft, A.; Osterod, F.; Fröhlich, R. *J. Org. Chem.* **1999**, *64*, 6425–6433.

Scheme 1. Helical Capsule-like Assembly through Charged Hydrogen Bonds



Addition of a solution of **1** in methanol to a solution of **2** in methanol resulted in a white suspension. The resulting solid was negligibly soluble in most organic solvents such as ethanol, chloroform, THF, and even DMF, but highly soluble in aqueous solvent. The ^1H NMR spectra of a 2:3 mixture of **1** and **2** in D_2O were simple, suggesting the formation of a symmetric structure. H-bond mediated association of **1** and **2** was determined to be reversible and fast on the NMR time scale. Therefore, the observed NMR resonances are averaged between the complex and each monomer, suggesting the formation of a discrete complex ($[\mathbf{1}_2\cdot\mathbf{2}_3]$) rather than higher oligomeric species.

The fact that the chiral proton of L-tartaric acid ($\mathbf{2}^L$) was strongly shifted upfield (4.76 to 4.31 ppm), coupled with the downfield shift of the aromatic and ethylene protons of **1** ($\Delta\delta = +0.31$ and $+0.36$ ppm, respectively) clearly shows that complexation occurs through the proton transfer from tartaric acid to the tris(imidazoline) base (Figure 1).

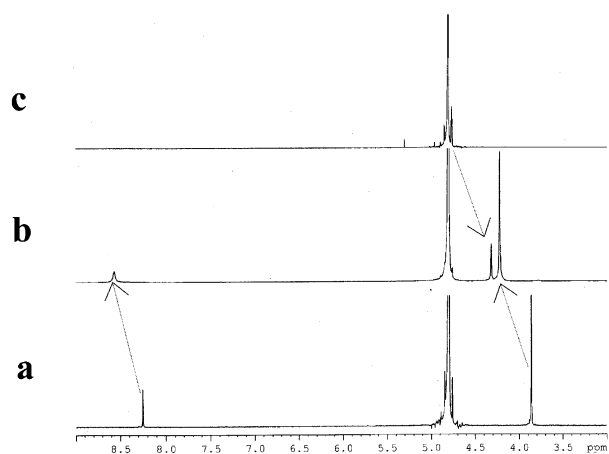


Figure 1. ^1H NMR spectra in D_2O at 298 K: (a) **1**, (b) $\mathbf{1}_2\cdot\mathbf{2}_3$ (2:3 molar ratio), and (c) $\mathbf{2}^L$. Peaks at 4.80 ppm are due to the residual solvent protons.

To confirm the formation of the dimeric ($[\mathbf{1}_2\cdot\mathbf{2}_3]$) supramolecular structures, we performed a mass spectrometric analysis for the complex. The crucial evidence for the formation of the dimeric structure was obtained by coldspray

ionization (CSI) mass spectra which clearly show molecular ion peaks and an appropriate fragmentation pattern in the concentration range of 0.1–100 mM (Figure 2).⁶

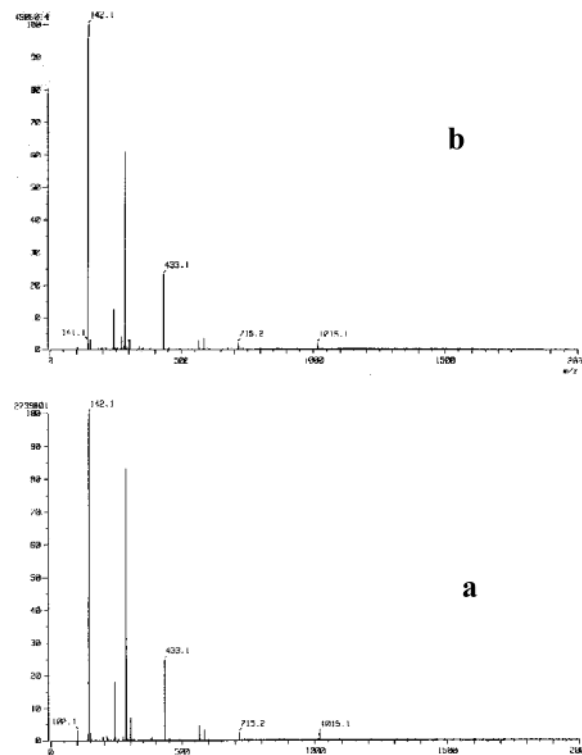


Figure 2. Cold spray ionization (CSI) mass spectra of the complex $[\mathbf{1}_2\cdot\mathbf{2}_3]$: (a) $[\mathbf{1}] = 200$ mM, $[\mathbf{2}] = 300$ mM, (b) $[\mathbf{1}] = 2$ mM, $[\mathbf{2}] = 3$ mM in water.

MALDI mass spectrometric analysis also corroborated the dimeric complex structure, where the isotope patterns at m/z 1058 ($[\mathbf{1}_2\cdot\mathbf{2}_3\cdot\text{CO}_2]^+$), 1080 ($[\mathbf{1}_2\cdot\mathbf{2}_3\cdot\text{CO}_2\cdot\text{Na}]^+$), and 1098 ($[\mathbf{1}_2\cdot\mathbf{2}_3\cdot\text{CO}_2\cdot\text{Na}\cdot\text{H}_2\text{O}]^+$) with 1 amu spacings are consistent with the calculated isotope distribution pattern corresponding to a monocharged molecular ion peak of the proposed dimeric structure. Additional support comes from a Job's plot analysis in D_2O , which indicates a 2:3 stoichiometry between **1** and **2**. Furthermore, concentration-dependent NMR spectra show little changes in ^1H NMR resonances upon increasing concentrations, and vapor pressure osmometry (VPO) data show the convergence of molecular weights, which exclude the possibility of self-aggregation or extensive association of 1D sheets at high concentrations. The complexation between **1** and **2** in a 1:1 ethanol/water mixture was driven by both enthalpy and entropy ($\Delta H_{\text{av}} = -3.64$ kcal/mol, $T\Delta S_{\text{av}} = +4.61$ kcal/mol at 30 °C) and was strong even in aqueous media ($\log K_{\text{av}} = 5.96$) (Figure 3).

Evidence for the helical structure of $[\mathbf{1}_2\cdot\mathbf{2}_3]$ comes from circular dichroism (CD) spectroscopic studies. When adding

(6) CSI-MS (positive ion, H_2O): m/z 142.1 ($[\mathbf{1}\cdot\mathbf{2}\text{H}]^{2+}$, 100%), 283.1 ($[\mathbf{1}\cdot\text{H}]^+$, 85%), 433.1 ($[\mathbf{1}\cdot\mathbf{2}^L\cdot\text{H}]^+$, 23%), 565.2 ($[\mathbf{1}_2\cdot\text{H}]^+$, 5%), 715.2 ($[\mathbf{1}_2\cdot\mathbf{2}^L\cdot\text{H}]^+$, 3%), 1015.1 ($[\mathbf{1}_2\cdot\mathbf{2}_3\cdot\text{H}]^+$, 2%); Sakamoto, S.; Fujita, M.; Kim, K.; Yamaguchi, K. *Tetrahedron* **2000**, *56*, 955–964.

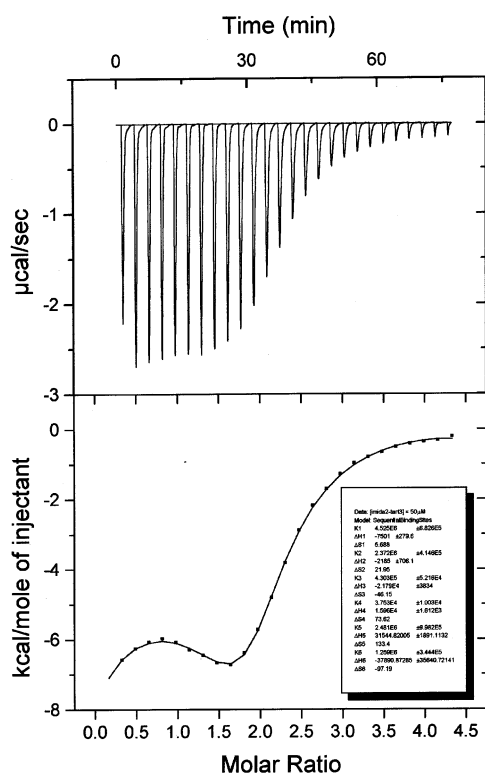


Figure 3. Titration of **1** with **2** by isothermal microcalorimetry under the condition of $[1]_0 = 50 \mu\text{M}$ and $[2]_0 = 3.9 \text{ mM}$ in $\text{H}_2\text{O}/\text{EtOH}$ (1:1, v/v) at $30 \text{ }^\circ\text{C}$.

2^L to a constant concentration ($10 \mu\text{M}$) of achiral tris-(imidazoline) (**1**) in aqueous ethanol, strong Cotton effects near the maxima of UV-vis absorbance of **1** appeared due to the chirality transfer of tartrate to **1**. Complementary signs were observed with 2^D as well: $\Delta A_{214 \text{ nm}} = +25.88 \text{ mdeg/cm}$ and -32.83 mdeg/cm for $1_2 \cdot 2^D_3$ and $1_2 \cdot 2^L_3$ at $[2]/[1] = 22$, respectively (Figure 4).

Complementary CD signs still remained even at $[2]/[1] = 3$ ($[1] = 16 \mu\text{M}$; $\Delta A_{214 \text{ nm}} = +19.36$ and -17.02 mdeg/

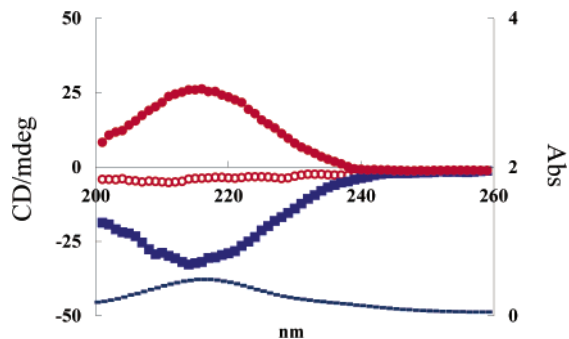


Figure 4. CD spectra of $[1_2 \cdot 2_3]$ and **1** in aqueous solvent (water/ethanol = 1:1, v/v) at $20 \text{ }^\circ\text{C}$. UV-vis absorbance of **1** (dashed line), CD spectra of $[1_2 \cdot 2_3]$ ($[1] = 10 \mu\text{M}$) after addition of 22 equiv of D- (filled circle) or L-tartaric acid (filled rectangle). Note no CD activity of **1** alone (open circle).

cm for $1_2 \cdot 2^D_3$ and $1_2 \cdot 2^L_3$, respectively). The fact that CD λ_{max} of $[1_2 \cdot 2_3]$ appears in almost the same wavelength as UV λ_{max} indicates that our system exists in a discrete dimeric form in solution without extensive self-association of 1D sheets through $\pi-\pi$ interaction.^{5c} These helical dimers $[1_2 \cdot 2^L_3]$ and $[1_2 \cdot 2^D_3]$ are affected by solvent polarity; upon increasing the percentage of ethanol, the CD intensity is slightly increased and the maxima of the Cotton effects are red-shifted. These phenomena are interpreted as follows: a charged hydrogen-bond mediated dimeric structure is favored in less polar solvent containing a larger quantity of ethanol giving rise to a self-assembled helical capsule. *Surprisingly, the multiple charged H-bonded helical assembly still remains intact even in pure water* (Figure 5).

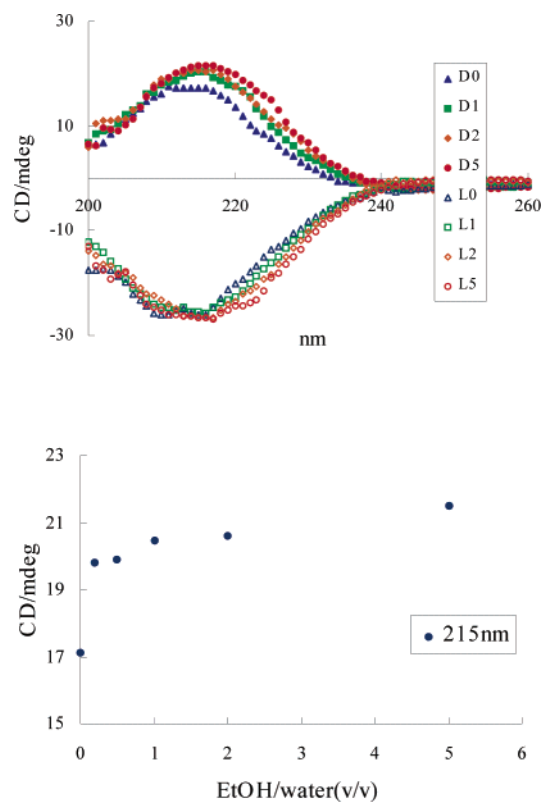


Figure 5. Solvent effect on (a) the CD spectra of the self-assembled structure, $[1_2 \cdot 2_3]$, where D0, D1, D2, and D5 mean 0:6, 1:5, 2:4, and 5:1 of ethanol/water solution of $[1_2 \cdot 2^D_3]$ in volume ratios, and the same notations apply for L0, L1, L2, and L5 of $[1_2 \cdot 2^L_3]$, and (b) its CD activity (ΔA) vs solvent composition at 215 nm under the conditions of $[1] = 5 \mu\text{M}$ and $[2]/[1] = 22$ in aqueous ethanol (1:1, v/v) at $20 \text{ }^\circ\text{C}$.

The absolute configuration for the induced helicity of $[1_2 \cdot 2_3]$ by chiral tartaric acid can be assigned by comparison with the signs of the Cotton effects for the crystal structures of similar helical complexes.⁷ $[1_2 \cdot 2^L_3]$ shows the same

(7) Kim, H.-J.; Moon, D.; Lah, M. S.; Hong, J.-I. *Angew. Chem., Int. Ed.* **2002**, *41*, 3174–3177. CCDC-182210 contains the supplementary crystallographic data for $M\text{-}[\text{Ag}_3\text{L}^*\text{Me}^{(S)}]^{3+}$, where $\text{L}^*\text{Me}^{(S)}$ stands for 1,3,5-tris[2-[4-(S)-methyl-1,3-oxazoline]]benzene.

negative Cotton effect as for the reference crystal structure of $M\text{-}[\text{Ag}_3\cdot\text{L}^{*Me(S)}_2]^{3+}$, while $[\mathbf{1}_2\cdot\mathbf{2}^D_3]$ shows the same positive Cotton effect as that of $P\text{-}[\text{Ag}_3\cdot\text{L}^{*Me(R)}_2]^{3+}$. Therefore, it can be concluded that M helicity is induced by L-tartaric acid to afford $M\text{-}[\mathbf{1}_2\cdot\mathbf{2}^L_3]$, while P helicity is induced by D-tartaric acid to afford $P\text{-}[\mathbf{1}_2\cdot\mathbf{2}^D_3]$.

To reason why L-tartaric acid induces M helicity in $[\mathbf{1}_2\cdot\mathbf{2}^L_3]$ (and vice versa), computational modeling for $[\mathbf{1}_2\cdot\mathbf{2}^L_3]$ was carried out to obtain a global minimized structure.⁸ The dimeric complex is plausibly formed by charged H-bonded triple clipping of three L-tartrate via twelve Coulombic H-bonds between the two parallel prestacked tris(imidazoliniums) (3.70 \AA) $\sim 30^\circ$ out of phase by $\pi\text{-}\pi$ interaction in water (Figure 6). While one carboxylate of **2** is hydrogen

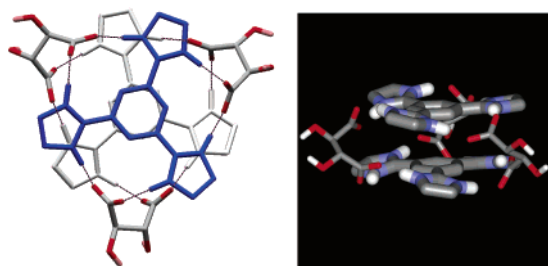


Figure 6. Energy-minimized structure of complex $M\text{-}[\mathbf{1}_2\cdot\mathbf{2}^L_3]$ in water. H-bonds viewed from the top are shown as dotted lines (left), and tris(imidazoliniums) from the side are represented as cylinders with tartrates as lines for clarity (right).

bonded with two imidazoliniums of **1** on one side, there is another carboxylate of **2** hydrogen bonded with two imidazoliniums of **1** on the other side that is parallel but $\sim 30^\circ$ out of phase. Chirality of L-tartaric acid seems to be transferred to the helicity of the complex through the directed hydrogen bonds to afford a left-handed structure, $M\text{-}[\mathbf{1}_2\cdot\mathbf{2}^L_3]$, which causes the same negative Cotton effect as in a similar

metal-mediated helical structure.⁷ Analyses of the H-bonding patterns of the calculated $M\text{-}[\mathbf{1}_2\cdot\mathbf{2}^L_3]$ and arbitrary $P\text{-}[\mathbf{1}_2\cdot\mathbf{2}^L_3]$ ⁹ gave insights into the understanding of the unidirectional helicity; the average bond angle and bond length of $\text{NH}\cdots\text{O}$ are 1.672 \AA and 168° in $M\text{-}[\mathbf{1}_2\cdot\mathbf{2}^L_3]$, whereas the values are 1.771 \AA and 145° in $P\text{-}[\mathbf{1}_2\cdot\mathbf{2}^L_3]$, which is not favored with regard to H-bonding due to the longer distance and narrower angle.¹⁰

In conclusion, we have demonstrated the first example of a novel H-bonded supramolecular chiral assembly with unidirectional helicity in aqueous solvent. These self-assembled supramolecules show strong Cotton effects, which are induced by chiral tartaric acid units, thus affording helical capsule-like structures of $M\text{-}[\mathbf{1}_2\cdot\mathbf{2}^L_3]$ and $P\text{-}[\mathbf{1}_2\cdot\mathbf{2}^D_3]$ from $\mathbf{2}^L$ and $\mathbf{2}^D$, respectively. Further studies involving the generation of an expanded cavity size, chiral recognition, separation, transport, and catalysis inside the cavity are underway.

Acknowledgment. Support of this work through a grant from the MOST (Grant No. M10213030001-02B1503-00210) is gratefully acknowledged. H.-J.K thanks the Ministry of Education for a BK 21 postdoctoral fellowship.

Supporting Information Available: ^1H and ^{13}C NMR spectra of $[\mathbf{1}_2\cdot\mathbf{2}^L_3]$, CD spectra, changes of the Cotton effect of $[\mathbf{1}_2\cdot\mathbf{2}_3]$ upon varying the ratios $[\mathbf{2}]/[\mathbf{1}]$, and solvent effect on CD spectra of $M\text{-}[\mathbf{1}_2\cdot\mathbf{2}^L_3]$ and $P\text{-}[\mathbf{1}_2\cdot\mathbf{2}^D_3]$, ESI, CSI, and MALDI mass spectra of $[\mathbf{1}_2\cdot\mathbf{2}^L_3]$, Job plot and VPO data for the complexation between **1** and **2**, and concentration-dependent ^1H NMR spectra of the complex. This material is available free of charge via the Internet at <http://pubs.acs.org>.

OL034155Y

(8) Conformational search was carried out with MacroModel 7.0 under Amber* force field in water: Mohamadi, F.; Richards, N. G. J.; Guida, W. C.; Liskamp, R.; Lipton, M.; Caufield, C.; Chang, G.; Hendrickson, T.; Still, W. C. *J. Comput. Chem.* **1990**, *11*, 440.

(9) The $P\text{-}[\mathbf{1}_2\cdot\mathbf{2}^L_3]$ structure was obtained by reversing the dihedral angle between the phenyl ring and the imidazoline ring to $+16.4^\circ$ from the lowest energy structure, $M\text{-}[\mathbf{1}_2\cdot\mathbf{2}^L_3]$.

(10) Taylor, R.; Kennard, O.; Versichel, W. *Acta Crystallogr.* **1984**, *B40*, 280–288.